Rotation - Torsion - Vibration Interaction in the Rotational Spectra of Isotopic Species of Ethyl Cyanide

H. M. Heise *, H. Mäder, and H. Dreizler

Abteilung Chemische Physik im Institut für Physikalische Chemie der Universität Kiel

(Z. Naturforsch. **31 a**, 1228–1241 [1976]; received July 14, 1976)

The measurements of the ground state rotational spectra of $CH_3CH_2C^{15}N$ and CH_3CD_2CN were extended to calculate the centrifugal distortion coefficients D_J, D_{JK} and D_K. The rotation-torsion-vibration interaction for these molecules including the normal species CH_3CH_2CN was studied in the rotational spectra of the first excited state of the methyl torsion and the CCN-in plane deformation. With respect to previous work a more detailed check of a model with five degrees of freedom comprising the overall rotation and the two lowest vibrations was possible.

Potential parameters were fitted simultaneously to the splittings of the rotational transitions in the two lowest excited vibrational states of the three isotopic molecules. The coefficients V_3 and V_6 of the Fourier expansion of the hindering potential for the torsion and an interaction constant V'_{3c} for the torsion and the CCN-in plane deformation were determined. Using these results it was possible to reproduce the frequencies of the torsional and CCN vibrations. With less success the torsional overtones could also be calculated.

Introduction

In a series of papers [1–6] we reported our investigation of **r**otation-**t**orsion-**v**ibration-(RTV)-interaction in asymmetric top molecules with a methyl group as internal rotor. The general aim is to study the cases in which the **r**igid **f**rame-**r**igid **t**op (RFRT) model [7, 8] is sufficient to evaluate the parameters for internal rotation or torsion and those in which a more extended RTV-model [1, 3] should be used.

The RTV-model differs from the RFRT-model by one additional vibrational degree of freedom. The main reason of the failure of RFRT-model is an interaction among torsional and vibrational levels depending partly on their energy differences. It should be pointed out that this interaction is present not only in molecules of the type CH_2FCOCH_3 (CH_3-torsion and CH_2F-torsion) [9], CH_3SSCD_3 (CH_3-torsion and SS-torsion) [6] or $CH_2ClCOCH_3$ (CH_3-torsion and CH_2Cl-torsion) [10], where this interaction still exists in the limit of harmonic force field. It has also to be considered in molecules such as CH_3SCN [5]. Here an interaction by higher than second order force constants between the CH_3-torsion and an CSC-in plane deformation vibration is observed.

Further more a detailed study of the RTV-Hamiltonian (2) (see below) reveals that "Coriolis"-type and more complicated interactions are included.

* This work is part of the thesis of H. M. Heise. Present address: School of Chemistry, University of Western Australia, Nedlands, Western Australia 6009.

Reprint requests to Prof. Dr. H. Dreizler, Abt. Chemische Physik, Institut für Physikalische Chemie der Universität Kiel, Olshausenstr. 40/60, *D-2300 Kiel*.

Up to now we applied the RTV-model to the molecules: CH_3SCN [2, 5], CH_3CH_2CN [4], CH_3COCN [11] and CH_3SSCD_3 [6]. These molecules cover a range of hindering potentials from 1.2 to 3 kcal/mole and a range of energy differences of the interacting torsional and vibrational levels from 4 to 50 cm^{-1}. The present study of the molecules CH_3CH_2CN, CH_3CD_2CN and $CH_3CH_2C^{15}N$ was initiated by the observation that the isotopic substitution varies the energy difference of the CH_3-torsion and the CCN-in plane deformation levels from approximately 4 cm^{-1} to 6 cm^{-1} and 8 cm^{-1} respectively. The rotational spectra should reflect these changes and provide a critical check of the applied Hamiltonian (2). We noticed in the preceding studies that a detailed knowledge of the vibrational spectrum and specially of the vibrational mode is important. Therefore, a very detailed study of the infrared and Raman spectra and a normal coordinate analysis of several isotopic species of CH_3CH_2CN was made, which will be published separately [12].

Experimental

The preparation of the samples of the isotopic species of ethyl cyanide was performed by a modified Kolbe reaction using the corresponding isotopic ethyl iodides and NaCN or $KC^{15}N$. The details of the preparation have been described elsewhere [4].

The microwave spectra were recorded with conventional 33 and 100 kHz Stark-modulation spectrographs [13, 14] employing phase stabilized BWO'S as radiation sources. The spectrographs were equipped with a 4.5 or 8 m absorption cell covered with a

cooling jacket. The measurements were carried out at a sample pressure of some mTorr and a temperature of approximately $-70\,^{\circ}C$.

For the assignment of the rotational transitions in the first excited state of the torsion and of the CCN-in plane deformation vibration radiofrequency-microwave double resonance (RF-MW-DR) experiments were carried out. The experimental set up is reported elsewhere [15] (for pump frequencies above 2.3 GHz the Rohde & Schwarz oscillator SLRC was used with amplitude modulation). In a preceding study of μ_a-transitions the B and C rotational constants were determined and the A constant estimated quite accurately. Then it was possible to calculate appropriate RF-pump frequencies first for the $J_{K-K+} - J'_{K'-K'+} = 3_{12} - 3_{13}$ pump transitions.

The signal μ_b-transition, $3_{03} - 3_{12}$, in the excited states of the isotopic molecules CH_3CD_2CN and $CH_3CH_2C^{15}N$ could be assigned without difficulty. These transitions were the key to the μ_b-spectra. For a demonstration of the simplicity of the RF-MW-DR-spectra a comparison with a Stark-modulated spectrum is given in Figure 1. In cases of overlapping due to other lines or Stark-satellites these experiments provided an important support to both measurement and assignment of the rotational transitions.

The spectra measured and/or analysed are given for the states indicated by the torsional and the vibrational quantum numbers $v_a\,v_q$ as follows:

$v_a\,v_q$	00	10	01
CH_3CH_2CN	Tab. 1, Ref. [4]	Tab. 12, Ref. [4]	Tab. 13, Ref. [4]
CH_3CD_2CN	Tab. 1	Tab. 2	Tab. 3
$CH_3CH_2C^{15}N$	Tab. 4	Tab. 5	Tab. 6

In Table 7 some frequencies are given for the RF-MW-DR experiments.

Table 1. Rotational transition (MHz) of the ground state $v_a\,v_q = 00$ of CH_3CD_2CN. a) Intensity weighted mean frequency of the rotational transitions without HFS, HFS see Ref. 4. b) Calculated with constants of Table 8.

Transition $J_{K-K+} - J'_{K'-K'+}$	experimental ν_{exp} [a]	calculated ν_{calc} [b]	$\nu_{exp} - \nu_{calc}$
$0_{00} - 1_{01}$	8 688.10	8 688.07	0.03
$1_{01} - 1_{10}$	17 855.12	17 855.11	0.01
$0_{00} - 1_{11}$	26 030.77	26 030.85	−0.08
$1_{01} - 2_{02}$	17 364.86	17 364.89	−0.03
$1_{10} - 2_{11}$	17 888.53	17 888.49	0.04
$1_{11} - 2_{12}$	16 863.77	16 863.82	−0.05
$2_{02} - 2_{11}$	18 378.78	18 378.71	0.07
$1_{01} - 2_{12}$	34 206.49	34 206.60	−0.11
$2_{20} - 3_{21}$	26 108.98	26 109.15	−0.17
$2_{02} - 3_{03}$	26 019.24	26 019.26	−0.02
$2_{11} - 3_{12}$	26 825.54	26 825.51	0.03
$2_{12} - 3_{13}$	25 288.61	25 288.66	−0.05
$2_{21} - 3_{22}$	26 064.60	26 064.44	0.16
$3_{03} - 3_{12}$	19 185.23	19 184.96	0.27
$3_{21} - 4_{22}$	34 855.17	34 855.13	0.04
$3_{03} - 4_{04}$	34 640.04	34 640.13	−0.09
$3_{12} - 4_{13}$	35 753.63	35 753.65	−0.02
$3_{13} - 4_{14}$	33 705.26	33 705.23	0.03
$3_{22} - 4_{23}$	34 743.75	34 743.60	0.15
$4_{04} - 4_{13}$	20 298.63	20 298.48	0.15
$4_{14} - 3_{21}$	20 689.14	20 688.99	0.15
$3_{13} - 4_{04}$	18 529.07	18 529.01	0.06
$4_{13} - 3_{22}$	15 510.69	15 510.84	−0.15
$5_{05} - 5_{14}$	21 751.09	21 751.04	0.05
$4_{14} - 5_{05}$	28 040.84	28 040.80	0.04
$6_{06} - 6_{15}$	23 579.82	23 580.14	−0.32
$5_{15} - 6_{06}$	37 670.19	37 670.25	−0.06

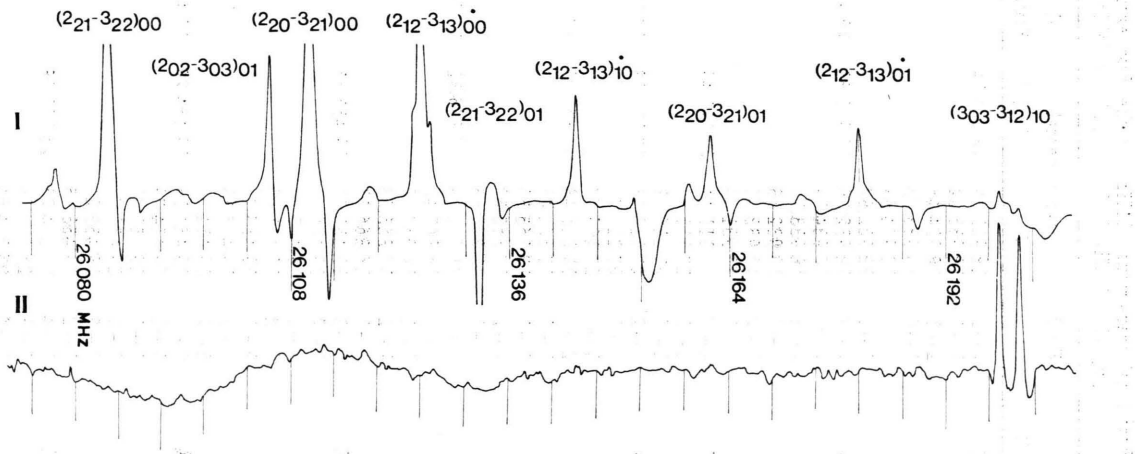

Fig. 1. I. Part of the Stark-modulated MW-spectrum of the $CH_3CH_2CN - CH_3CH_2C^{15}N$ mixture. Stark-field 340 V/cm. II. RF-MW-DR-spectrum of the same region recorded with increased sensitivity. Pumptransition: $CH_3CH_2C^{15}N$, $v_a\,v_q = 10$, $3_{12} - 3_{13} = 2712.5$ MHz. Output power of SLRC (Rohde & Schwarz) RF-generator approx. 2 Watts. Markers distance 5.6 MHz. $v_a\,v_q = 00$ ground state, $v_a\,v_q = 10$ first excited torsional state, $v_a\,v_q = 01$ first excited CCN-in plane deformation state. Transitions not marked by an asterisk belong to $CH_3CH_2C^{15}N$.

Table 2. Rotational transitions (MHz) of the first excited torsional state $v_a v_q = 10$ of CH_3CD_2CN. a), b) see Table 1.

Transition $J_{K-K+} - J'_{K'-K'+}$		$F-F'$	experimental ν_{HFS}	experimental ν_{exp} [a]	calculated ν_{calc} [b]	$\nu_{exp}-\nu_{calc}$
$1_{01}-1_{10}$	E	2−2	18 933.86	18 934.11		
		1−1	18 935.52			
		2−1	18 934.45			
		1−0	18 933.86			
		1−2	18 934.83			
		0−1	18 932.87			
	A	2−2	18 932.58	18 932.83	18 932.79	0.04
		1−1	18 934.19			
		2−1	18 933.17			
		1−0	18 932.58			
		1−2	18 933.62			
		0−1	18 931.63			
$0_{00}-1_{11}$	E	1−2	27 111.44	27 111.49		
		1−1	27 111.83			
		1−0	27 110.71			
	A	1−2	27 110.33	27 110.38	27 110.48	−0.10
		1−1	27 110.71			
		1−0	27 109.67			
$1_{01}-2_{02}$		2−3	17 366.43	17 366.39	17 366.34	0.05
		1−2	17 366.43			
		0−1	17 365.50			
		2−2	17 365.50			
		1−1	17 368.05			
$1_{11}-2_{12}$		2−3	16 866.53	16 866.32	16 866.39	−0.07
		1−2	16 865.45			
		0−1	16 867.60			
		2−2	16 865.88			
		1−1	16 866.53			
$2_{02}-2_{11}$	E	3−3	19 455.50	19 455.55		
		2−2	19 456.06			
		1−1	19 455.00			
		3−2	19 455.00			
		2−1	19 456.75			
		2−3	19 456.53			
		1−2	19 454.35			
	A	3−3	19 454.13	19 454.28	19 454.25	0.03
		2−2	19 454.79			
		1−1	19 453.73			
		3−2	19 453.73			
		2−3	19 455.26			
		1−2	19 453.05			
$2_{20}-3_{21}$	E	3−4	26 104.25	26 103.98		
		2−3	26 103.08			
		1−2	26 104.84			
		3−3	26 104.25			
		2−2	26 103.08			

Continued Table 2

Transition $J_{K-K+} - J'_{K'-K'+}$		$F-F'$	experimental ν_{HFS}	experimental ν_{exp} [a]	calculated ν_{calc} [b]	$\nu_{exp}-\nu_{calc}$
$2_{02}-3_{03}$		3−4	26 023.42	26 023.44	26 023.42	0.02
		2−3	26 023.42			
		1−2	26 023.42			
		3−3	26 022.33			
		2−2	26 025.04			
$2_{12}-3_{13}$		3−4	25 293.06	25 293.00	25 293.16	−0.16
		2−3	25 292.80			
		1−2	25 293.06			
		3−3	25 292.25			
		2−2	25 294.21			
$2_{21}-3_{22}$	E	3−4	26 071.82	26 071.55		
		2−3	26 070.66			
		1−2	26 072.43			
		3−3	26 071.82			
		2−2	26 070.66			
	A	3−4	26 067.01	26 066.76	26 066.98	−0.22
		2−3	26 065.89			
		1−2	26 067.62			
		3−3	26 067.01			
		2−2	26 065.89			
$3_{03}-3_{12}$	E	4−4	20 257.29	20 257.42		
		3−3	20 257.70			
		2−2	20 257.29			
	A	4−4	20 255.96	20 256.08	20 255.98	0.10
		3−3	20 256.35			
		2−2	20 255.96			
$3_{21}-4_{22}$	E	4−5	34 851.20			
		2−3	34 851.20			
		3−3	34 851.20			
	A	4−5	34 852.40	34 852.23	34 852.37	−0.14
		3−4	34 851.89			
		2−3	34 852.40			
		4−4	34 851.89			
		3−3	34 852.40			
$3_{03}-4_{04}$		4−5	34 649.36	34 649.36	34 649.35	0.01
		3−4	34 649.36			
		2−3	34 649.36			
		4−4	34 648.24			
		3−3	34 650.75			
$3_{12}-4_{13}$				35 754.42	35 754.42	0.00
$3_{13}-4_{14}$		4−5	33 712.51	33 712.51	33 712.41	0.10
		3−4	33 712.50			
		2−3	33 712.50			
		4−4	33 711.44			
		3−3	33 713.75			

Continued Table 2

Transition $J_{K-K+}-J'_{K'-K'+}$		$F-F'$	experimental ν_{HFS}	ν_{exp} [a]	calculated ν_{calc} [b]	$\nu_{\mathrm{exp}}-\nu_{\mathrm{calc}}$
$3_{22}-4_{23}$	E	4−5	34 749.90			
		2−3	34 749.90			
		3−3	34 749.90			
	A	4−5	34 748.39	34 748.23	34.747.92	0.31
		3−4	34 747.91			
		2−3	34 748.39			
		4−4	34 747.91			
		3−3	34 748.39			
$4_{04}-4_{13}$	E	5−5	21 362.45	21 362.54		
		4−4	21 362.75			
		3−3	21 362.45			
	A	5−5	21 360.99	21 361.09	21 361.05	0.04
		4−4	21 361.30			
		3−3	21 360.99			
$3_{13}-4_{04}$	E	4−5	17 456.80	17 456.74		
		3−4	17 456.61			
		2−3	17 456.80			
	A	4−5	17 457.64	17 457.58	17 457.47	0.11
		3−4	17 457.46			
		2−3	17 457.64			
$5_{05}-5_{14}$	E	6−6	22 800.88	22 800.95		
		5−5	22 801.11			
		4−4	22 800.88			
	A	6−6	22 799.31	22 799.38	22 799.38	0.00
		5−5	22 799.55			
		4−4	22 799.31			
$4_{14}-5_{05}$	E			26 978.72		
	A			26 979.44	26 979.37	0.07
$6_{06}-6_{15}$	E	7−7	24 608.06	24 608.13		
		6−6	24 608.28			
		5−5	24 608.06			
	A	7−7	24 606.33	24 606.39	24 606.45	−0.06
		6−6	24 606.54			
		5−5	24 606.33			
$5_{15}-6_{06}$	E			36 626.16		
	A			36 626.77	36 626.88	−0.11

Table 3. Rotational transitions (MHz) of the first excited CCN-in plane deformation state $v_\alpha\, v_g=01$ of CH_3CD_2CN. a), b) see Table1.

Transition $J_{K-K+}-J'_{K'-K'+}$		$F-F'$	experimental ν_{HFS}	ν_{exp} [a]	calculated ν_{calc} [b]	$\nu_{\mathrm{exp}}-\nu_{\mathrm{calc}}$
$0_{00}-1_{01}$		1−2	8 703.10	8 702.95	8 702.94	0.01
		1−1	8 702.12			
		1−0	8 704.68			
$1_{01}-1_{10}$	E	2−2	16 830.33	16 830.56		
		1−1	16 831.91			
		2−1	16 830.89			
		1−0	16 830.33			
		1−2	16 831.25			
		0−1	16 829.39			
	A	2−2	16 830.62	16 830.88	16 830.85	0.03
		1−1	16 832.26			
		2−1	16 831.25			
		1−0	16 830.62			
		1−2	16 831.64			
		0−1	16 829.72			
$0_{00}-1_{11}$	E	1−2	25 020.68	25 020.72		
		1−1	25 021.01			
		0−1	25 020.04			
	A	1−2	25 021.01	25 021.07	25 021.18	−0.11
		1−1	25 021.39			
		0−1	25 020.38			
$1_{01}-2_{02}$		2−3	17 393.92	17 393.85	17 393.88	−0.03
		1−2	17 393.92			
		0−1	17 392.88			
		2−2	17 392.88			
		1−1	17 395.58			
$1_{10}-2_{11}$		2−3	17 918.57	17 918.37	17 918.29	0.08
		1−2	17 917.53			
		0−1	17 919.74			
		2−2	17 918.20			
		1−1	17 918.20			
$1_{11}-2_{12}$		2−3	16 893.19	16 892.93	16 893.06	−0.13
		1−2	16 892.14			
		0−1	16 894.20			
		2−2	16 892.54			
		1−1	16 892.54			
$2_{02}-2_{11}$	E	3−3	17 354.90	17 355.07		
		2−2	17 355.60			
		1−1	17 354.56			
		3−2	17 354.56			
		2−1	17 356.32			
		1−2	17 353.87			
	A	3−3	17 355.26	17 355.41	17 355.41	0.15
		2−2	17 355.95			
		1−1	17 354.90			
		3−2	17 354.90			

Continued Table 3

Transition $J_{K-K+}-J'_{K'-K'+}$		$F-F'$	experimental ν_{HFS}	ν_{exp} [a]	calculated ν_{calc} [b]	$\nu_{exp}-\nu_{calc}$
		2−1	17 356.59			
		2−3	17 356.32			
		1−2	17 354.22			
$1_{01}-2_{12}$	E	2−3	33 210.77	33 210.80		
		1−2	33 211.09			
		2−2	33 210.10			
	A	2−3	33 211.09	33 211.13	33 211.30	−0.17
		1−2	33 211.44			
		2−2	33 210.41			
$2_{20}-3_{21}$		3−4	26 155.83	26 155.58	26 155.33	0.25
		2−3	26 154.72			
		1−2	26 156.44			
		3−3	26 155.83			
		2−2	26 154.72			
$2_{02}-3_{03}$		3−4	26 060.84	26 060.86	26 060.88	−0.02
		2−3	26 060.84			
		1−2	26 060.84			
		3−3	26 059.71			
		2−2	26 062.38			
$2_{11}-3_{12}$		3−4	26 869.81	26 869.72	26 869.66	0.06
		2−3	26 869.50			
		1−2	26 869.81			
		3−3	26 869.12			
		2−2	26 870.48			
$2_{12}-3_{13}$		3−4	25 331.93	25 331.86	25 331.99	−0.13
		2−3	25 331.66			
		1−2	25 331.93			
		3−3	25 331.02			
		2−2	25 332.95			
$3_{03}-3_{12}$	E	4−4	18 163.87	18 163.98		
		3−3	18 164.22			
		2−2	18 163.87			
	A	4−4	18 164.22	18 164.34	18 164.03	0.31
		3−3	18 164.59			
		2−2	18 164.22			
$3_{21}-4_{22}$		4−5	34 919.79	34 919.61	34 919.20	0.41
		3−4	34 919.23			
		2−3	34 919.79			
		4−4	34 919.23			
		3−3	34 919.79			
$3_{03}-4_{04}$				34 692.18	34 692.21	−0.03
$3_{12}-4_{13}$		4−5	35 811.42	35 811.42	35 811.45	−0.03
		3−4	35 811.42			
		2−3	35 811.42			
		4−4	35 810.60			
		3−3	35 812.34			

Continued Table 3

Transition $J_{K-K+}-J'_{K'-K'+}$		$F-F'$	experimental ν_{HFS}	ν_{exp} [a]	calculated ν_{calc} [b]	$\nu_{exp}-\nu_{calc}$
$3_{13}-4_{14}$		4−5	33 761.78	33 761.79	33 762.02	−0.23
		3−4	33 761.78			
		2−3	33 761.78			
		4−4	33 760.84			
		3−3	33 763.15			
$3_{22}-4_{23}$		4−5	34 800.58	34 800.42	34 800.70	−0.28
		3−4	34 800.09			
		2−3	34 800.58			
		4−4	34 800.09			
		3−3	34 800.58			
$4_{04}-4_{13}$	E	5−5	19 283.18	19 283.28		
		4−4	19 283.49			
		3−3	19 283.18			
	A	5−5	19 283.49	19 283.60	19 283.27	0.33
		4−4	19 283.83			
		3−3	19 283.49			
$3_{13}-4_{04}$	E	4−5	19 604.19			
		2−3	19 604.19			
	A	4−5	19 603.93	19 603.86	19 603.69	0.17
		3−4	19 603.71			
		2−3	19 603.93			
$5_{05}-5_{14}$	E	6−6	20 746.32	20 746.42		
		5−5	20 746.62			
		4−4	20 746.32			
	A	6−6	20 746.62	20 746.72	20 746.59	0.13
		5−5	20 746.92			
		4−4	20 746.62			
$4_{14}-5_{05}$	E			29 118.77		
	A			29 118.51	29 118.41	0.10
$6_{06}-6_{15}$	E	7−7	22 592.47			
		5−5	22 592.47			
	A	7−7	22 592.80	22 592.88	22 593.35	−0.47
		6−6	22 593.04			
		5−5	22 592.80			
$5_{15}-6_{06}$	E			38 742.79		
	A			38 742.51	38 742.58	−0.07

Table 4. Rotational transitions (MHz) of the ground state $v_a\, v_q = 00$ of $CH_3CH_2C^{15}N$. a) Calculated with constants of Table 8.

Transition $J_{K_-K_+} - J'_{K'_-K'_+}$	experimental ν_{exp}	calculated ν_{calc} [a]	$\nu_{exp} - \nu_{calc}$
$0_{00} - 1_{01}$	8 694.31	8 694.28	0.03
$1_{01} - 1_{10}$	23 422.15	23 421.98	0.17
$0_{00} - 1_{11}$	31 660.92	31 661.00	−0.08
$1_{01} - 2_{02}$	17 381.76	17 381.79	−0.03
$1_{10} - 2_{11}$	17 843.97	17 843.92	0.05
$1_{11} - 2_{12}$	16 933.36	16 933.40	−0.04
$2_{02} - 2_{11}$	23 884.16	23 884.11	0.05
$1_{01} - 2_{12}$	39 899.96	39 900.12	−0.16
$2_{20} - 3_{21}$	26 110.23	26 110.37	−0.14
$2_{02} - 3_{03}$	26 055.77	26 055.78	−0.01
$2_{11} - 3_{12}$	26 761.44	26 761.49	−0.05
$2_{12} - 3_{13}$	25 395.73	25 395.77	−0.04
$2_{21} - 3_{22}$	26 083.68	26 083.57	0.11
$3_{03} - 3_{12}$	24 589.95	24 589.83	0.12
$3_{21} - 4_{22}$	34 839.57	34 839.49	0.08
$3_{03} - 4_{04}$	34 709.49	34 709.52	−0.03
$3_{12} - 4_{13}$	35 673.65	35 673.71	−0.06
$3_{13} - 4_{14}$	33 853.09	33 853.04	0.05
$3_{22} - 4_{23}$	34 772.67	34 772.56	0.11
$4_{04} - 4_{13}$	25 554.23	25 554.02	0.21
$4_{14} - 3_{21}$	37 128.22	37 128.12	0.10
$3_{13} - 4_{04}$	12 851.32	12 851.20	0.12
$4_{13} - 3_{22}$	32 542.34	32 542.44	−0.10
$5_{05} - 5_{14}$	26 796.30	26 796.20	0.10
$4_{14} - 5_{05}$	22 334.69	22 334.62	0.07
$6_{06} - 6_{15}$	28 339.76	28 340.07	−0.31
$5_{15} - 6_{06}$	31 961.26	31 961.35	−0.09

Analysis of Spectra

Ground State

The ground state spectra have been analysed in a preceding publication [16]. The r_s-structure of Table 11, Ref. [16] was used with some modifications for the RTV-model.

In addition a centrifugal distortion analysis was carried out according to the following expression for the rotational energy $E_{J_{K_-K_+}}$ for a near prolate top:

$$E_{J_{K_-K_+}} = E^0_{J_{K_-K_+}}(A,B,C) - D_J J^2(J+1)^2 - D_{JK} J(J+1)\langle P_a^2\rangle - D_K \langle P_a^4\rangle \quad (1)$$

with $E^0_{J_{K_-K_+}}$ rigid rotor energy, D_J, D_{JK}, D_K centrifugal distortion parameters, $\langle P_a^n\rangle$ expectation value of the operator P_a^n in the rotational state $J_{K_-K_+}$.

The results are given in Table 8. The calculated frequencies are compared with the measured ones in Tables 1 and 4.

Excited States

Before applying the RTV-model the excited state spectra (A-species) have been checked for consistency of measurements and assignment by a centrifugal distortion analysis according to Equation (1). The resulting parameters are given in Table 8. D_K was set to zero as only transitions with $\max(K_-) = 1$ were measured. The errors of this analysis are shown in Tables 2, 3, 5, 6 and Tables 12 and 13 of Reference [4].

Figure 2 shows some typical sections of the rotational spectrum of $CH_3CH_2C^{15}N$. The most important features of the spectrum to be interpreted are the splittings of the excited states $v_a\, v_q = 01$ and 10. As the ground state lines $v_a\, v_q = 00$ are not split, it should be noticed that the $v_a\, v_q = 01$ lines are doublets ($v_a = 0!$). Their splittings vary considerably with the isotopic species, depending on the energy difference of the CH_3-torsional and CCN-in plane deformation vibrational levels.

Table 5. Rotational transitions (MHz) of the first excited torsional state $v_a\, v_q = 10$ of $CH_3CH_2C^{15}N$. a) see Table 4.

Transition $J_{K_-K_+} - J'_{K'_-K'_+}$		experimental ν_{exp}	calculated ν_{calc} [a]	$\nu_{exp} - \nu_{calc}$
$1_{01} - 1_{10}$	E	25 042.61		
	A	25 040.03	25 040.46	−0.43
$0_{00} - 1_{11}$	E	33 284.47		
	A	33 282.25	33 282.80	−0.55
$1_{01} - 2_{02}$		17 382.67	17 383.15	0.48
$1_{10} - 2_{11}$		17 841.50	17 841.94	−0.44
$1_{11} - 2_{12}$		16 937.14	16 937.12	0.02
$2_{02} - 2_{11}$	E	25 501.46		
	A	25 498.91	25 499.25	−0.34
$2_{20} - 3_{21}$	E	26 104.05		
$2_{02} - 3_{03}$		26 058.68	26 058.90	−0.22
$2_{11} - 3_{12}$		26 758.50	26 758.65	−0.15
$2_{12} - 3_{13}$		25 402.01	25 401.47	0.54
$2_{21} - 3_{22}$	E	26 092.88		
	A	26 086.07	26 084.80	1.27
$3_{03} - 3_{12}$	E	26 201.39		
	A	26 198.87	26 199.00	−0.13
$3_{21} - 4_{22}$	E	34 829.46		
	A	34 833.48	34 836.02	−2.54
$3_{03} - 4_{04}$		34 716.18	34 715.70	0.48
$3_{12} - 4_{13}$	E	35 671.03		
	A	35 670.74	35 670.16	0.58
$3_{13} - 4_{14}$		33 862.63	33 860.84	1.79
$3_{22} - 4_{23}$	E	34 776.84		
$4_{04} - 4_{13}$	E	27 156.11		
	A	27 153.44	27 153.47	−0.03
$3_{13} - 4_{04}$	E	11 228.60		
	A	11 230.56	11 231.10	−0.54
$5_{05} - 5_{14}$	E	28 383.72		
	A	28 380.89	28 380.71	0.18
$4_{14} - 5_{05}$	E	20 715.47		
	A	20 717.27	20 717.64	−0.37
$6_{06} - 6_{15}$	E	29 906.31		
	A	29 903.30	29 902.76	0.54
$5_{15} - 6_{06}$	E	30 350.49		
	A	30 352.14	30 352.00	0.14

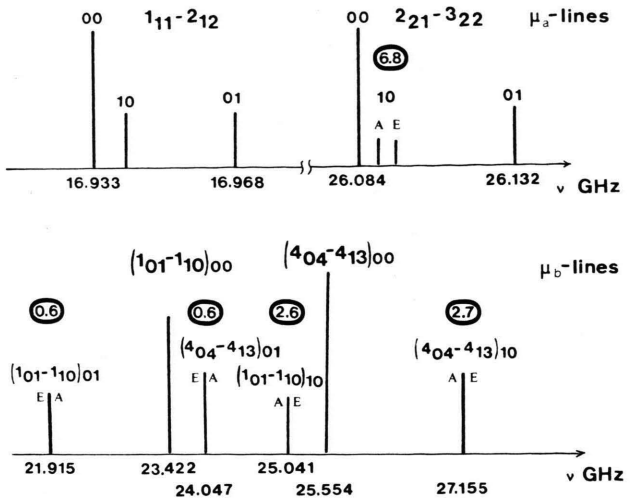

Fig. 2. Typical sections of the rotational spectrum of $CH_3CH_2C^{15}N$. Transitions are signed by $(J_{K-K+}-J'K'_-K'_+)$ and $v_a v_q$. The torsional line splittings (MHz) are given in circles.

Table 6. Rotational transitions (MHz) of the first excited CCN-in plane deformation state $v_a v_q=01$ of $CH_3CH_2C^{15}N$. a) see Table 4.

Transition $J_{K-K+}-J'_{K'-K'+}$		experimental ν_{exp}	calculated ν_{calc} [a]	$\nu_{exp}-\nu_{calc}$
$0_{00}-1_{01}$		8 711.39	8 711.34	0.05
$1_{01}-1_{10}$	E	21 915.05		
	A	21 915.65	21 915.60	0.05
$0_{00}-1_{11}$	E	30 171.99		
	A	30 172.57	30 172.65	−0.08
$1_{01}-2_{02}$		17 415.46	17 415.45	0.01
$1_{10}-2_{11}$		17 876.86	17 876.75	0.11
$1_{11}-2_{12}$		16 968.05	16 968.16	−0.11
$2_{02}-2_{11}$	E	22 376.47		
	A	22 377.06	22 376.90	0.16
$1_{01}-2_{12}$	E	38 428.68		
	A	38 429.27	38 429.47	−0.20
$2_{20}-3_{21}$		26 161.54	26 161.38	0.16
$2_{02}-3_{03}$		26 105.03	26 105.09	−0.06
$2_{11}-3_{12}$		26 810.44	26 810.37	0.07
$2_{12}-3_{13}$		25 447.37	25 447.56	−0.19
$2_{21}-3_{22}$		26 132.70	26 132.85	−0.15
$3_{03}-3_{12}$	E	23 081.90		
	A	23 082.48	23 082.18	0.30
$3_{21}-4_{22}$		34 909.40	34 909.03	0.37
$3_{12}-4_{13}$		35 738.06	35 738.19	−0.13
$3_{13}-4_{14}$		33 921.19	33 921.44	−0.25
$4_{04}-4_{13}$	E	24 047.12		
	A	24 047.68	24 047.29	0.39
$3_{13}-4_{04}$	E	14 417.33		
	A	14 416.86	14 416.60	0.26
$5_{05}-5_{14}$	E	25 292.52		
	A	25 293.11	25 292.94	0.17
$4_{14}-5_{05}$	E	23 908.25		
	A	23 907.76	23 907.62	0.14
$6_{06}-6_{15}$	E	26 843.14		
	A	26 843.67	26 844.21	−0.54
$5_{15}-6_{06}$	E	33 536.53		
	A	33 535.99	33 536.11	−0.12

Table 7. Pump frequencies (MHz) of the RF-MW-DR experiments.

CH_3CD_2CN	$v_a v_q=10$	$3_{12}-3_{13}$	3 063.2
		$3_{22}-2_{21}$, E	55.9
	$v_a v_q=01$	$3_{12}-3_{13}$	3 076.6
$CH_3CH_2C^{15}N$	$v_a v_q=10$	$3_{12}-3_{13}$	2 712.5
		$3_{22}-2_{21}$, A	30.4
	$v_a v_q=01$	$3_{22}-2_{21}$, E	44.5
		$3_{12}-3_{13}$	2 727.0

Hamiltonian

The RTV-model is described in an "Eckart-system" by the following Hamiltonian (2) for a molecule with a symmetry plane (y, z) and an in plane vibration. A detailed discussion is given in [3, 4]. There are implied two basic assumptions:

I. The internal rotor has at least C_3-symmetry about its internal rotation axis.

II. The configuration of the internal rotor is not affected by the vibration.

The Hamiltonian of the RTV-model is:

$$\begin{aligned}\mathcal{H} = {} & A(q)P_z^2 + B(q)P_y^2 + C(q)P_x^2 \\ & + D_{yz}(q)\,(P_y P_z + P_z P_y) \\ & - 2\,Q_y(q)\,p_\alpha P_y - 2\,Q_z(q)\,p_\alpha P_z \\ & + F(q)\,p_\alpha^2 + \frac{V_3}{2}(1-\cos 3\alpha) + \frac{V_6}{2}(1-\cos 6\alpha) \\ & + \tfrac{1}{4}\,[M(q)\,p_q^2 + p_q^2\,M(q)] + \tfrac{1}{2}\,k_{2q}\,q^2 \\ & + W(q) + \tfrac{1}{2}\,k_{3q}\,q^3 + \tfrac{1}{2}\,k_{4q}\,q^4 \qquad (2)^* \\ & + V'_{3c}\,q(1-\cos 3\alpha) + V''_{3c}\,q^2(1-\cos 6\alpha)\end{aligned}$$

where

P_g operator of the total angular momentum component with respect to the g-axis of the "Eckart-system" $g = x, y, z$,

p_α operator of the torsional angular momentum,

p_q operator of the vibrational momentum,

q vibrational coordinate,

α torsional angle.

$$\begin{aligned} A(q) &= (h/8\pi^2)\,(I_{yy} - \lambda_y^2\,I_\alpha)/r\Delta \\ B(q) &= (h/8\pi^2)\,(I_{zz} - \lambda_z^2\,I_\alpha)/r\Delta \\ C(q) &= (h/8\pi^2)/I_{xx} \\ D_{yz}(q) &= -(h/8\pi^2)\,(I_{yz} - \lambda_y\,\lambda_z\,I_\alpha)/r\Delta \\ Q_y(q) &= (h/8\pi^2)\,(\lambda_y\,I_{zz} - \lambda_z\,I_{yz})/r\Delta \\ Q_z(q) &= (h/8\pi^2)\,(\lambda_z\,I_{yy} - \lambda_y\,I_{yz})/r\Delta \end{aligned}$$

* Erratum to Ref. [3]: M^0 in (41i) should be replaced by $\frac{1}{2}M^0$; $\frac{1}{2}V''_{3c}$ should be replaced by V''_{3c}.

Table 8. Rotational constants and centrifugal distortion parameters (MHz) for the rotational spectra according to (1). For $v_a\, v_q = 10$ and 01, D_K was set to zero. In brackets standard errors of the fit.

	CH_3CH_2CN [4]					
$v_a\, v_q$	00		10		01	
A	27663.751	(0.074)	29794.20	(1.48)	25656.24	(0.33)
B	4714.157	(0.016)	4713.81	(0.38)	4717.47	(0.09)
C	4235.135	(0.011)	4239.66	(0.27)	4296.95	(0.06)
D_J	0.0031	(0.0003)	0.029	(0.008)	0.001	(0.002)
D_{JK}	−0.041	(0.001)	−0.160	(0.031)	0.120	(0.008)
D_K	0.546	(0.019)	0		0	
	CH_3CD_2CN					
$v_a\, v_q$	00		10		01	
A	21943.195	(0.070)	23021.49	(0.07)	20296.07	(0.10)
B	4600.206	(0.015)	4599.55	(0.02)	4607.78	(0.03)
C	4087.873	(0.011)	4088.84	(0.01)	4095.17	(0.02)
D_J	0.0026	(0.0003)	0.0008	(0.0004)	0.0043	(0.0006)
D_{JK}	−0.020	(0.002)	−0.071	(0.003)	0.024	(0.004)
D_K	0.252	(0.015)	0		0	
	$CH_3CH_2C^{15}N$					
$v_a\, v_q$	00		10		01	
A	27541.965	(0.067)	29161.55	(0.48)	26044.19	(0.11)
B	4574.777	(0.015)	4573.59	(0.12)	4582.83	(0.03)
C	4119.516	(0.011)	4121.18	(0.08)	4128.53	(0.02)
D_J	0.0028	(0.0003)	0.006	(0.003)	0.0043	(0.0007)
D_{JK}	−0.041	(0.0002)	−0.049	(0.021)	0.032	(0.005)
D_K	0.549	(0.014)	0		0	

$$F(q) = (h/8\pi^2)/r\, I_a$$

$$M(q) = (h/4\pi^2)/G^{-1}$$

$$r(q) = 1 - I_a(\lambda_y^2 I_{zz} - 2\lambda_y \lambda_z I_{yz} + \lambda_z^2 I_{yy})/\Delta$$

$$\Delta(q) = I_{yy} I_{zz} - I_{yz}^2$$

$I_{gg}(q)$ momentum of inertia about the g-axis of the "Eckart-system" $(g = x, y, z)$,

$I_{yz}(q)$ product of inertia,

$\lambda_g(q)$ direction cosine of the internal rotation axis to the g-axis $(g = y, z)$,

I_a moment of inertia of the top about its symmetry axis,

$G^{-1}(q) = \sum_k m_k(\partial \mathfrak{r}_k/\partial q)^2$ "reduced mass" for the vibration (m_k mass, and $\mathfrak{r}_k$ position vector of atom k).

The term $W(q)$ arises from the translation of the classical to the quantum mechanical Hamiltonian. The potential energy in H (2) contains a three- and sixfold term for the pure torsion (V_3, V_6), harmonic, cubic and quartic force constants for the vibration (k_{2q}, k_{3q}, k_{4q}) and two potential coupling terms, V_{3c}'' and V_{3c}'', for torsion-vibration interaction. These potential coupling terms represent cubic and quartic force constants in the limit of small amplitudes of the torsional angle.

Kinetic Coefficients

For the numerical treatment of the Hamiltonian (2) the q-dependent coefficients of its kinetic part are expanded in power series of q up to second order.

$$Y = Y^0 + Y' q + Y'' q^2 \qquad (3)$$

with Y for A, B, C, D_{yz}, Q_y, Q_z, F, M and W. The expansion coefficients in (3) are molecular constants depending on atomic masses, molecular structure and vibrational mode. Higher order expansion coefficients have been found to be negligible.

From a normal coordinate analysis [12] we determined the vibrational mode as given in Table 9 and shown in Figure 3.

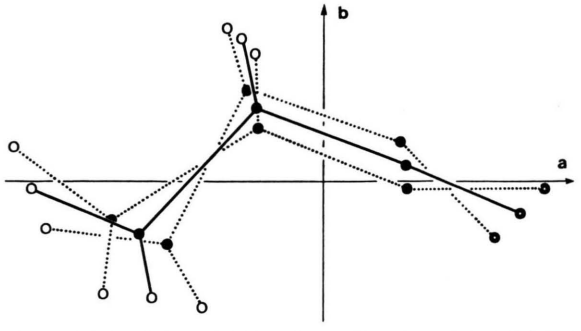

Fig. 3. Mode of the CCN-in plane vibration of CH_3CH_2CN. The vibrational coordinate q is positive if the angle CCC increases.

Table 9. Vibrational modes determined by a normal coordinate analysis [17]. The vibrational coordinate q is defined by the synchronous changes of the angles ∢CCN, ∢CCC and ∢HCH of the CH_2-group. q is positive for increasing ∢CCC.

	Δ ∢CCN	Δ ∢CCC	Δ ∢HCH
CH_3CH_2CN	1.000	0.399	−0.200
CH_3CD_2CN	1.000	0.398	−0.195
$CH_3CH_2C^{15}N$	1.000	0.397	−0.199

Using this mode together with the r_s-structure (Table 11 of Ref. [16]), which was modified to obtain a C_3-symmetric CH_3-group,

$$r_{C-H} = 1.091\ \text{Å}, \quad \text{∢HCC} = 110.47^\circ$$

and the atomic masses [18] the kinetic coefficients (3) of the Hamiltonian (2) were calculated *. They are given in Table 10. The transformation from the instantaneous principal axis system to the "Eckart-system" was performed by using Eq. (53) of Ref. [3]

$$\bar{\vartheta} = \int_{q_0}^{q} [\bar{H}_x(q')/\bar{I}_{xx}(q')]\, dq' \qquad (4)$$

with $\bar{\vartheta}$ angle between the instantaneous principal axis system and the "Eckart-system",

$$\bar{H}_x = \sum m_k (\mathfrak{r}_k \times \partial \mathfrak{r}_k/\partial q)_x ,$$

$\bar{I}_{xx}$ moment of inertia, both calculated in the instantaneous principal axis system.

For the calculation of the coefficients (3) a fifth order polynomial was least squares fitted to 11 points. These points are given by the deformation of the molecule according to the mode (Table 9) by changing q from −5 to +5 degrees in steps of 1 degree. An estimate of the mean amplitude of the CCN-in plane deformation by $\sqrt{\langle v_q | q^2 | v_q \rangle} = \sqrt{3\,M^0/2\,\omega}$ for $v_q = 1$ gives approximately 7 degrees. By changing the range of deformation to ±10 degrees the effective rotational constant A for $v_a\, v_q = 10$ varies by 150 kHz and the splittings of the rotational lines by 100 Hz in the most unfavourable case.

Potential Coefficients

For the potential coefficients of the Hamiltonian (2) the following procedure was applied. The force constant k_{2q} * was determined from the measured CCN-in plane deformation frequencies of Table 11 by

$$k_{2q} = \omega^2/M^0 .$$

They agree for the three isotopic molecules within approximately 1%. It was numerically tested that the

* Program ANMA 5.F4 author U. Andresen and H. Mäder.

* The force constant k_{2q} differs by definition from that used in the normal coordinate analysis [12].

		CH_2CH_3CN	CH_3CD_2CN	$CH_3CH_2C^{15}N$	CD_3CH_2CN
A^0	GHz	30.107158	23.380290	29.927041	26.767960
B^0	GHz	4.804628	4.687681	4.660793	4.342946
C^0	GHz	4.246262	4.098250	4.130176	3.807494
D^0_{yz}	GHz	−0.449944	−0.339535	−0.433454	−0.722711
Q^0_y	GHz	−3.836896	−3.737802	−3.736213	−3.597546
Q^0_z	GHz	20.742376	15.734697	20.483364	19.325867
F^0	GHz	176.880	173.220	176.560	96.201
M^0	GHz·rad²	65.623	64.431	64.255	56.462
A'	GHz/rad	29.642760	18.482796	29.567686	27.945624
B'	GHz/rad	−2.036667	−1.850984	−1.968792	−1.956541
C'	GHz/rad	−1.109965	−0.979054	−1.087441	−1.086723
D'_{yz}	GHz/rad	−2.870407	−2.752584	−2.865513	−2.597504
Q'_y	GHz/rad	1.028289	0.983178	0.966465	0.808994
Q'_z	GHz/rad	33.223540	22.911606	33.199790	30.561752
F'	GHz/rad	28.152	19.072	28.108	26.396
W'	GHz/rad	−14.630	−15.040	−15.360	−14.410
M'	GHz·rad	31.560	27.657	31.791	29.328
A''	GHz/rad²	23.784017	12.552967	23.859040	24.358328
B''	GHz/rad²	2.249163	2.131895	2.194069	2.181887
C''	GHz/rad²	0.981428	0.911640	0.971959	0.922516
D''_{yz}	GHz/rad²	−2.336392	−1.733650	−2.280568	−2.446515
Q''_y	GHz/rad²	−4.515813	−3.927187	−4.436857	−4.415042
Q''_z	GHz/rad²	25.177040	13.602124	25.220395	25.406212
F''	GHz/rad²	30.894	19.158	30.957	29.999
W''	GHz/rad²	12.600	10.000	11.200	6.500
M''	GHz	−1.259	−5.304	−1.177	2.464

Table 10. Kinetic coefficients of the Hamiltonian (2). The rotational constants A^0, B^0, C^0 differ from A, B, C by definition. Conversion factor 505.376 AMU Å²·GHz, atomic masses [18].

CH_3CH_2CN	206.9 ± 0.5
CH_3CD_2CN	204.7 ± 0.5
$CH_3CH_2C^{15}N$	203.4 ± 0.8

Table 11. Measured frequencies [cm^{-1}] of the CCN-in plane deformation vibration.

terms with the coefficients M', M'', F', F'', W' and W'' do not influence the energy of the vibrational level $v_q = 1$ by more than 0.1 cm^{-1}, a value which is less than the experimental error. Neither do the values of the potential coefficients V'_{3c} and V''_{3c} shift the energy of the vibrational level $v_q = 1$ by more than 0.1 cm^{-1} if they are in the order of the final result (see Table 15).

The higher order force constants k_{3q} and k_{4q} could not be determined reliably from the vibrational spectra and were assumed to be zero. Thus the pure vibrational part of the Hamiltonian (2) reduces to

$$\mathcal{H}_v = \tfrac{1}{2} M^0 p_q^2 + \tfrac{1}{2} k_{2q} q^2 \qquad (5)$$

with $k_{2q} = \omega^2 / M^0$. With all other coefficients of the Hamiltonian (2) determined as described above the potential parameters V_3, V_6, V'_{3c} and V''_{3c} remain to be calculated from the experimental data.

We used the A – E-splittings of transitions up to $J = 4$* of CH_3CH_2CN, CH_3CD_2CN and $CH_3CH_2C^{15}N$ (Table 12, 13, 14) simultaneously for a least squares

* Limited by the capacity of the computer.

Table 12. Observed and calculated A – E splittings (MHz) of rotational transitions in the excited states $v_\alpha v_q = 10$ and 01 of CH_3CH_2CN. [a] $\Delta = (\nu_E - \nu_A)_{exp} - (\nu_E - \nu_A)_{calc}$, $\% = \Delta / (\nu_E - \nu_A)_{exp}$ in per cent.

Transition $J_{K-K+} - J'_{K'-K'+}$	$v_\alpha v_q$	$\nu_E - \nu_A$ exp	$\nu_E - \nu_A$ calc	Δ [a]	% [a]
$0_{00} - 1_{11}$	10	2.64	2.64	0.00	0.0
$1_{01} - 1_{10}$		2.99	3.00	−0.01	0.3
$2_{02} - 2_{11}$		2.92	2.93	−0.01	0.3
$3_{03} - 3_{12}$		2.90	2.98	−0.08	2.8
$2_{21} - 3_{22}$		6.99	7.07	−0.08	1.1
$4_{04} - 4_{13}$		3.08	3.08	0.00	0.0
$3_{21} - 4_{22}$		−4.11	−4.09	−0.02	0.5
$3_{22} - 4_{23}$		4.59	4.54	0.05	1.1
$3_{12} - 4_{13}$		0.36	0.33	0.03	8.3
$4_{14} - 5_{05}$		−2.20	−2.21	−0.01	0.5
$5_{05} - 5_{14}$		3.27	3.23	0.04	1.2
$5_{15} - 6_{06}$		−2.06			
$6_{06} - 6_{15}$		3.44			
$0_{00} - 1_{11}$	01	−0.91	−0.86	−0.05	5.5
$1_{01} - 1_{10}$		−0.95	−0.86	−0.09	9.5
$1_{01} - 2_{12}$		−0.94	−0.85	−0.09	9.6
$2_{02} - 2_{11}$		−0.92	−0.87	−0.05	5.4
$3_{03} - 3_{12}$		−0.95	−0.88	−0.07	7.4
$4_{04} - 4_{13}$		−0.99	−0.90	−0.09	9.1
$4_{14} - 5_{05}$		0.86	0.82	0.04	4.7
$5_{05} - 5_{14}$		−1.00	−0.92	−0.08	8.0
$5_{15} - 6_{06}$		0.84	—		
$6_{06} - 6_{15}$		−1.03	—		

Table 13. Observed and calculated A – E splittings (MHz) of rotational transitions in the excited states $v_\alpha v_q = 10$ and 01 of CH_3CD_2CN. [a] see Table 12.

Transition $J_{K-K+} - J'_{K'-K'+}$	$v_\alpha v_q$	$\nu_E - \nu_A$ exp	$\nu_E - \nu_A$ calc	Δ [a]	% [a]
$0_{00} - 1_{11}$	10	1.11	1.27	−0.16	14.4
$1_{01} - 1_{10}$		1.28	1.41	−0.13	10.2
$2_{02} - 2_{11}$		1.27	1.41	−0.14	11.0
$3_{03} - 3_{12}$		1.34	1.47	−0.13	9.7
$2_{21} - 3_{22}$		4.79	5.01	−0.22	4.6
$4_{04} - 4_{13}$		1.45	1.57	−0.12	8.3
$3_{13} - 4_{04}$		−0.84	−0.98	0.14	16.7
$3_{21} - 4_{22}$		−1.20	−1.32	0.12	10.0
$3_{22} - 4_{23}$		1.51	1.69	−0.18	11.9
$4_{14} - 5_{05}$		−0.72	−0.85	0.13	18.1
$5_{05} - 5_{14}$		1.57	1.70	−0.13	8.3
$5_{15} - 6_{06}$		−0.61			
$6_{06} - 6_{15}$		1.74			
$0_{00} - 1_{11}$	01	−0.35	−0.37	0.02	5.7
$1_{01} - 1_{10}$		−0.32	−0.37	0.05	15.6
$1_{01} - 2_{12}$		−0.33	−0.36	0.03	9.1
$2_{02} - 2_{11}$		−0.34	−0.37	0.03	8.8
$3_{03} - 3_{12}$		−0.36	−0.38	0.02	5.6
$3_{13} - 4_{04}$		0.26	0.36	−0.10	38.5
$4_{04} - 4_{13}$		−0.32	−0.39	0.07	21.9
$4_{14} - 5_{05}$		0.26	0.35	−0.09	34.6
$5_{05} - 5_{14}$		−0.30	−0.39	0.09	30.0
$5_{15} - 6_{06}$		0.28	—		
$6_{06} - 6_{15}$		−0.33	—		

Table 14. Observed and calculated A – E splittings (MHz) of rotational transitions in the excited states $v_\alpha v_q = 10$ and 01 of $CH_3CH_2C^{15}N$. [a] see Table 12.

Transition $J_{K-K+} - J'_{K'-K'+}$	$v_\alpha v_q$	$\nu_E - \nu_A$ exp	$\nu_E - \nu_A$ calc	Δ [a]	% [a]
$0_{00} - 1_{11}$	10	2.22	2.17	0.05	2.3
$1_{01} - 1_{10}$		2.58	2.52	0.06	2.3
$2_{02} - 2_{11}$		2.55	2.46	0.09	3.5
$3_{03} - 3_{12}$		2.52	2.51	0.01	0.4
$2_{21} - 3_{22}$		6.81	6.78	0.03	0.4
$3_{13} - 4_{04}$		−1.96	−1.90	−0.06	3.1
$4_{04} - 4_{13}$		2.67	2.61	0.06	2.2
$3_{21} - 4_{22}$		−4.02	−4.09	0.07	1.7
$3_{12} - 4_{13}$		0.29	0.31	−0.02	6.9
$4_{14} - 5_{05}$		−1.80	−1.76	−0.04	2.2
$5_{05} - 5_{14}$		2.83	2.75	0.08	2.8
$5_{15} - 6_{06}$		−1.65			
$6_{06} - 6_{15}$		3.01			
$0_{00} - 1_{11}$	01	−0.58	−0.45	−0.13	22.4
$1_{01} - 1_{10}$		−0.60	−0.45	−0.15	25.0
$1_{01} - 2_{12}$		−0.59	−0.45	−0.14	23.7
$2_{02} - 2_{11}$		−0.59	−0.45	−0.14	23.7
$3_{03} - 3_{12}$		−0.58	−0.46	−0.12	20.7
$3_{13} - 4_{04}$		0.47	0.44	0.03	6.4
$4_{04} - 4_{13}$		−0.56	−0.46	−0.10	17,9
$4_{14} - 5_{05}$		0.49	0.43	0.06	12.2
$5_{05} - 5_{14}$		−0.59	−0.46	−0.13	22.0
$5_{15} - 6_{06}$		0.54	—		
$6_{06} - 6_{15}$		−0.53	—		

Table 15. Final set of the potential coefficients V_3, V_6, V'_{3c} and other parameters for the molecules CH_3CH_2CN, CH_3CD_2CN and $CH_3CH_2C^{15}N$. The results of this work are compared to those of preceding publications.

	this work	4 ×	19 ××	20 ××
V_3	3226 ± 10 cal/mole (1128.2 ± 3.4 cm^{-1})	3188 ± 5 cal/mole	3005 ± 150 cal/mole	3002 ± 150 cal/mole
V_6	−172 ± 0.5 cal/mole (−60.2 ± 0.2 cm^{-1})	−190 ± 3 cal/mole	—	—
V'_{3c}	−1421 ± 134 cal/(mole·rad) (−497.0 ± 46.7 cm^{-1}/rad)	—	—	—
λ^0_z	0.6780	0.6672	0.6676	$\alpha=\lambda_a(I_a/I_a)$ 0.1528 +
λ^0_y	−0.7351	−0.7449	−0.7445	$\beta=\lambda_b(I_a/I_b)$ −0.0368 +
F^0	176.881 GHz	179.19 GHz	174.4 GHz	91.34 GHz
I_a	3.159 AMU·Å²	3.105 AMU·Å²	3.197 AMU·Å²	
$S=\frac{4V_3}{9F^0}$	85.0	82.9	81.5	153.15 (76.6) ++

× From RTV-model applied to CH_3CH_2CN only. The vibrational mode and structure differ from this work. These values corrected (see Ref. 4).
×× From $v_a=1$ μa-transitions of CH_3CH_2CN by RFRT-model.
××× From $v_a=3$ μa-transitions of CD_3CD_2CN by RFRT-model.
+ λ_z and λ_y not given.
++ Mass corrected by m_D/m_H.

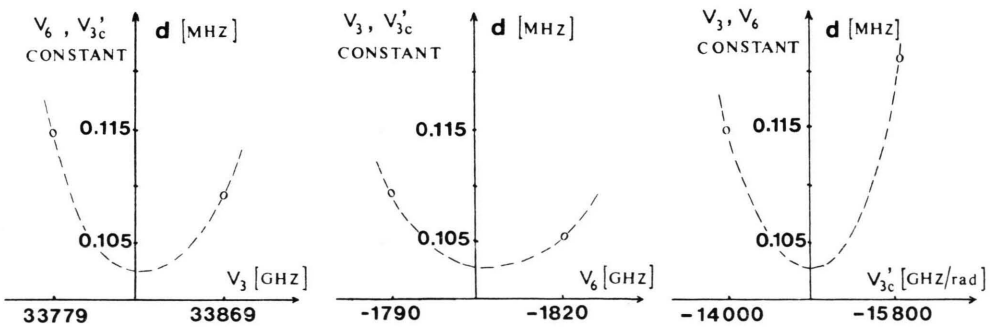

Fig. 4. Mean square error d [MHz] of the calculated A−E splittings of Table 10, 11 and 12 for the molecules CH_3CH_2CN, CH_3CD_2CN and $CH_3CH_2C^{15}N$. V_3, V_6 and V'_{3c} are varied independently. The minimum values are given in Table 15.

fit of V_3, V_6, V'_{3c} and V''_{3c}. It was noticed that the splittings are by an order of magnitude less sensitive to V''_{3c} than to V'_{3c}, so we set $V''_{3c}=0$. The mean partial derivatives are **:

$$\overline{\partial\Delta\nu/\partial V_3} \approx 0.8\cdot10^{-3}\ \text{MHz/GHz},$$
$$\overline{\partial\Delta\nu/\partial V_6} \approx 0.1\cdot10^{-2}\ \text{MHz/GHz},$$
$$\overline{\partial\Delta\nu/\partial V'_{3c}} \approx 0.5\cdot10^{-4}\ \text{MHz/(GHz rad}^{-1}),$$
$$\overline{\partial\Delta\nu/\partial V''_{3c}} \approx 0.6\cdot10^{-5}\ \text{MHz/(GHz rad}^{-2}).$$

The final result is the set of V_3, V_6 and V'_{3c} given in Table 15. The set applies to all three molecules CH_3CH_2CN, CH_3CD_2CN and $CH_3CH_2C^{15}N$ simultaneously. It should be mentioned that V'_{3c} is correlated to V_3 as can be seen from the correlation coefficients of Table 16. The observed and calculated splittings are compared in Tables 12 – 14. Table 15 gives also a comparison with the preceding work based on the RTV-[4] and RFRT-model [19, 20]. Figure 4 demonstrates the stability of the least squares fit.

Table 16. Correlation coefficients for V_3, V_6 and V'_{3c}.

V_3	1.000		
V_6	−0.414	1.000	
V'_{3c}	−0.980	0.307	1.000

** Defined to be $\frac{1}{N}\sum_i^N\left|\frac{\partial\Delta\nu}{\partial X}\right|$ for N splittings and $X=V_3$, V_6, V'_{3c}, V''_{3c}.

Model calculations were performed for potential parameters considering a value for V'_{3c} which was opposite in sign to the value of Table 15. We did not find any hint for another reasonable minimum in the least squares fit.

Numerical Procedure

The numerical calculations were performed according to the flow diagram of Fig. 3, Reference [3]. The basis set of free rotor functions was limited by $|m|_{\max} = 24\ (25)$ for the A (E) species. Torsional functions $U_{v_\alpha\sigma}(\alpha)$ up to $v_\alpha = 6$ and vibrational functions $H_{v_q}(q)$ up to $v_q = 5$ were used for the torsion-vibration problem. The complete rotation-torsion-vibration Hamiltonian was set up with 18 torsion-vibration functions $\Phi v_\alpha \sigma v_q(\alpha, q)$ up to $v_\alpha + v_q = 5$. So the splittings could be calculated * with an accuracy of approximately 10 kHz using double word precision of the PDP10.

Discussion

As it can be seen from Table 15 the results of different publications dot not agree in the range of experimental errors. The experimental information was much less intensive in the compared publications [4, 19, 20]. We believe that the measurements of μ_b-transitions in the excited states are necessary for an analysis of this kind. The knowledge of the vibrational spectra is essential for the RTV-model. Furthermore the methods of analysis differed by the applied Hamiltonian [19, 20] or by numerical values of coefficients [4].

Using the set of parameters of Table 15 the RTV-model reproduces the torsional frequencies [12] reasonably well as shown in Table 17.

For this comparison CD_3CH_2CN was included. (The torsional fine structure of the rotational spectrum of this molecule could not be resolved. Thus it could not be included in the RTV-analysis.)

It should be pointed out that the fit of the splittings of the rotational transitions is quite good, but the frequencies of the corresponding transitions are badly reproduced. An indication of this problem is given in Table 18, where experimental and calculated rotational constants are compared.

* Programs MRTVD1. F4 to MRTVD4. F4, author H. Mäder.

Table 17. Calculated and measured transitions [cm^{-1}] for CH_3-torsion and CCN-in plane deformation. The torsional frequencies have been determined from combination bands [$\tau(CH_3) + \nu_a(CH_3)$]. For CD_3CH_2CN these transitions were measured directly in FIR [12]. The CCN-in plane transitions were used to determined k_{2q} of the Hamiltonian (2). The calculated frequencies were obtained using this k_{2q} and all other model parameters. For the CCN-in plane deformation frequencies this is a check for the approximate evaluation of k_{2q}.

		exp.		calc.
CH_3CH_2CN	$\tau(1-0)$	210.7		211.9
	$\tau(2-1)$	201.4		204.6
	$\tau(3-2)$	187.8	A	193.5
			E	192.8
	$\tau(4-3)$	170.5	A	172.9
			E	179.4
	$\delta(1-0)$	206.9		206.7
CH_3CD_2CN	$\tau(1-0)$	210.2		209.7
	$\tau(2-1)$	200.4		202.5
	$\tau(3-2)$	187.4	A	191.7
			E	191.1
	$\tau(4-3)$	170.2	A	172.3
			E	178.0
	$\delta(1-0)$	204.7		204.4
$CH_3CH_2C^{15}N$	$\tau(1-0)$	—		211.7
	$\tau(2-1)$	—		204.2
	$\tau(3-2)$	—	A	193.3_3
			E	193.2_6
	$\tau(4-3)$	—	A	172.9
			E	178.8
	$\delta(1-0)$	203.4		203.2
CD_3CH_2CN	$\tau(1-0)$	159.8		157.7
	$\tau(2-1)$	154.2		154.4
	$\tau(3-2)$	147.5		149.9
	$\tau(4-3)$	139.7		144.0
	$\delta(1-0)$	192.5		192.3

This seems to be a general problem that was also observed many times when using the RFRT model for the determination of hindering potentials.

Some other preliminary evaluation procedures of the experimental data have been discussed in Reference [17].

We did not yet systematically study the influence of the assumed structure on the results, but we took the r_0-structure Table 9, Ref. [4], as a basis of a test. This r_0-structure differs from the modified r_s-structure (see above) mainly in the structural parameters of the C – H bonds. As a consequence I_a changes to $I_a = 3.105$ AMU · Å^2. The vibrational mode was kept as given in Table 9. The A – E splittings calculated with the set of potential parameters of Table 15 change quite sensitively. As an example for CH_3CH_2CN:

$(0_{00} - 1_{11})_{01}$ -0.86 MHz $\rightarrow$ -0.69 MHz,
$(0_{00} - 1_{11})_{10}$ 2.64 MHz $\rightarrow$ 2.52 MHz,
$(2_{21} - 3_{22})_{10}$ 7.07 MHz $\rightarrow$ 7.56 MHz.

Table 18. Differences between experimental and calculated effective rotational constants (MHz) of ground ($v_a v_q = 00$) and excited ($v_a v_q = 10$ and 01) states. They have been calculated from the $1_{01}-1_{10}$, $0_{00}-1_{01}$ and $0_{00}-1_{11}$ transitions:

$$A_{v_a v_q} = \tfrac{1}{2}\{(1_{01}-1_{10})_{v_a v_q} + (0_{00}-1_{11})_{v_a v_q}\}$$
$$B_{v_a v_q} = (0_{00}-1_{01})_{v_a v_q} - C_{v_a v_q}$$
$$C_{v_a v_q} = (0_{00}-1_{11})_{v_a v_q} - A_{v_a v_q}$$

		exp.	calc.
CH_3CH_2CN	$A_{00}-A_{10}$	−2 130.82	−1 170.27
	$B_{00}-B_{10}$	1.84	10.15
	$C_{00}-C_{10}$	−4.22	0.95
	$A_{00}-A_{01}$	2 007.54	951.59
	$B_{00}-B_{01}$	−3.27	−20.22
	$C_{00}-C_{01}$	−11.68	−16.67
CH_3CD_2CN	$A_{00}-A_{10}$	−1 078.66	−606.38
	$B_{00}-B_{10}$	0.95	8.92
	$C_{00}-C_{10}$	−0.65	2.45
	$A_{00}-A_{01}$	1 016.97	470.93
	$B_{00}-B_{01}$	−7.58	−20.57
	$C_{00}-C_{01}$	−7.27	−13.62
$CH_3CH_2C^{15}N$	$A_{00}-A_{10}$	−1 619.61	−756.58
	$B_{00}-B_{10}$	1.72	9.29
	$C_{00}-C_{10}$	1.72	3.27
	$A_{00}-A_{01}$	1 497.42	537.18
	$B_{00}-B_{01}$	−8.01	−23.20
	$C_{00}-C_{01}$	−9.07	−14.24

We believe that these changes cannot be related to the change of I_a alone. In conclusion, a precise structure is necessary for an analysis of this kind.

To estimate the influence of the vibrational mode, the modified r_s-structure was used and the mode changed to $\Delta \sphericalangle$ CCN : $\Delta \sphericalangle$ CCC : $\Delta \sphericalangle$ HCH = 1 : 0.505 : 0.193. (This mode resulted from a preliminary normal coordinate analysis [17].) The representative splittings change as follows:

$$(0_{00}-1_{11})_{01} \quad -0.86\ \text{MHz} \rightarrow -0.83\ \text{MHz},$$
$$(0_{00}-1_{11})_{10} \quad 2.64\ \text{MHz} \rightarrow 2.65\ \text{MHz},$$
$$(2_{21}-3_{22})_{10} \quad 7.07\ \text{MHz} \rightarrow 6.98\ \text{MHz}.$$

Although $\Delta \sphericalangle$ CCC was changed by more than 25% the influence on the splittings is smaller than 4%. This seems favourable since the accuracy of the determination of the mode is inferior to that of the structure. To test the influence of the CCN-in plane vibration the frequency was altered within the experimental accuracy from 206.8 cm^{-1} to 206.5 cm^{-1} for CH_3CH_2CN. The modified r_s-structure and the mode of Table 9 was used. The change of the representative line splittings are:

$$(0_{00}-1_{11})_{01} \quad -0.86\ \text{MHz} \rightarrow -0.80\ \text{MHz},$$
$$(0_{00}-1_{11})_{10} \quad 2.64\ \text{MHz} \rightarrow -2.59\ \text{MHz},$$
$$(2_{21}-3_{22})_{10} \quad 7.07\ \text{MHz} \rightarrow 7.09\ \text{MHz}.$$

According to our general experience [4] the splittings of μ_b-transitions change more sensibly than those of μ_a-transitions.

We believe that neither reasonable changes in the structure nor in the mode or the CCN-in plane vibrational frequency can remove the still existing discrepancy in the calculation of the frequencies (not the splittings) of the rotational transitions. For illustration Fig. 5 gives the potential surface of the RTV-

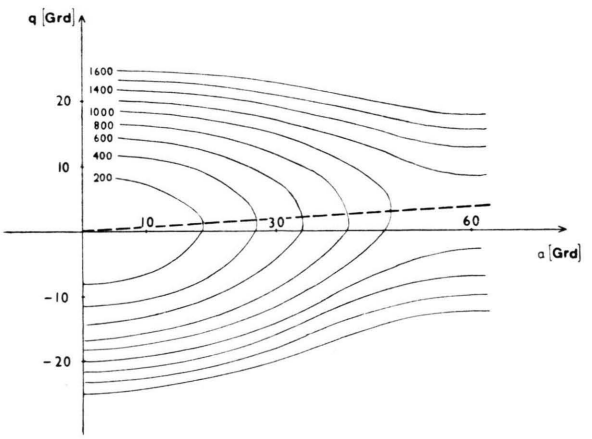

Fig. 5. Potential surface $V(\alpha, q)$ of the torsion-vibration for CH_3CH_2CN.

$$V(\alpha, q) = \tfrac{1}{2} V_3(1-\cos 3\alpha) + \tfrac{1}{2} V_6(1-\cos 6-\alpha) + \tfrac{1}{2} k_{2q} q^2 + V'_{3c}\, q(1-\cos 3\alpha)\ .$$

$V_3 = 1128.2\ cm^{-1}$, $V_6 = -60.2\ cm^{-1}$, $V'_{3c} = 497.0\ cm^{-1}/rad$, $k_{2q} = 19\,556\ cm^{-1}/rad^2$, α torsional angle, q vibrational coordinate, – – – minimum energy path of internal rotation.

model as determined in this work. A consequence of the potential coupling (V'_{3c}) is that the minimum energy path for the internal rotation is curvilinear in the α, q plane. By this picture the RTV-model is related to the r_e-relaxation method [21] where the minimum energy path is introduced parametrically. Thus the number of degrees of freedom (three rotational and one torsional) is maintained in the r_e-relaxation method.

Finally we want to stress that the analysis of torsional fine structures of rotational spectra in excited torsional states should be made with great care. If there is a low lying vibrational energy level, RTV-interaction ought to be considered. It was shown in this work, that the RTV-model interprets the three lowest states $v_a v_q$ reasonably well for three isotopic forms of CH_3CH_2CN.

Whenever possible the hindering potential V_3 should be determined from the torsional fine structure of the ground state. In principle the RTV-model is a first step from the RFRT-model to a general treatment [22, 23]. With the available experimental data and a reasonable use of present computers a general treatment of a model with $3N-6$ internal degrees of freedom seems out of sight.

We particularly thank Dr. R. Schwarz for setting up the RF-MW-DR apparatus. – We thank Dr. F. Scappini and Dr. F. Winther for reading the manuscript, the members of our group for many helpful discussions. The work was supported by the Deutsche Forschungsgemeinschaft and Fonds der Chemie. The calculations were performed on the PDP10 computer of the Rechenzentrum der Universität Kiel.

[1] H. Dreizler, Z. Naturforsch. **23 a**, 1077 [1968].
[2] H. Dreizler and A. Mirri, Z. Naturforsch. **23 a**, 1313 [1968].
[3] H. Mäder, U. Andresen, and H. Dreizler, Z. Naturforsch. **28 a**, 1163 [1973].
[4] H. Mäder, H. M. Heise, and H. Dreizler, Z. Naturforsch. **29 a**, 164 [1974].
[5] U. Andresen and H. Dreizler, Z. Naturforsch. **29 a**, 797 [1974].
[6] M. Kuhler, L. Charpentier, D. Sutter, and H. Dreizler, Z. Naturforsch. **29 a**, 1335 [1974].
[7] C. C. Lin and J. D. Swalen, Rev. Mod. Physics **31**, 841 [1959].
[8] H. Dreizler, Fortschritte der Chem. Forschung **10**, 59 [1968].
[9] E. Saegebarth and N. C. Krisher, J. Chem. Phys. **52**, 3555 [1970].
[10] T. Ikeda, R. F. Curl, and H. Karlsson, J. Mol. Spectrosc. **53**, 101 [1974]; H. Karlsson, Dissertation, Stockholm 1976.
[11] F. Scappini and H. Dreizler, to be published.
[12] H. M. Heise, H. Lutz, F. Winther, and H. Dreizler, to be published.
[13] H. D. Rudolph, Z. Angew. Physik **13**, 401 [1961].
[14] U. Andresen and H. Dreizler, Z. Angew. Physik **30**, 207 [1970].
[15] R. Schwarz, H. Dreizler, and A. Guarnieri, Z. Naturforsch. **30 a**, 180 [1975].
[16] H. M. Heise, H. Lutz, and H. Dreizler, Z. Naturforsch. **29 a**, 1345 [1974].
[17] H. M. Heise, Dissertation Kiel 1976.
[18] W. Gordy and R. L. Cook, Microwave Molecular Spectra, Interscience Publishers, New York 1970, p. 651, 653.
[19] V. W. Laurie, J. Chem. Phys. **26**, 678 [1957].
[20] Y. S. Li and J. R. Durig, J. Mol. Spectrosc. **54**, 296 [1975].
[21] A. Bauder and Hs. H. Günthard, J. Mol. Spectrosc. **60**, 290 [1976].
[22] B. Kirtman, J. Chem. Phys. **37**, 2516 [1962].
[23] C. R. Quade, J. Chem. Phys. **44**, 2512 [1966].